Direct imaging of tunneling from a potential well

Mathew Tomes[1,*], Kerry J. Vahala[2], Tal Carmon[1]

[1]*Electrical Engineering and Computer Science, University of Michigan, Ann Arbor, Michigan, 48109, USA*
[2]*Applied Physics Department, California Institute of Technology, 1200 E. California Blvd, Pasadena, California, 91125, USA*
**tomesmat@umich.edu*

Abstract: We experimentally map the wavefunction in the vicinity of a radial potential well. We photograph light intensity near the tunneling region as well as measure the spiraling phase structure via interference with a reference wave. This spiraling phase structure is required for conservation of angular momentum. The experimental image reveals the non-intuitive emission of light from a region in space that is empty of material and relatively far from the device.

OCIS codes: (230.5750) Resonators; (140.3945) Microcavities

References and links

1. I. Newton, *Opticks: or, a treatise of the reflections, refractions, inflections and colours of light* (Printed for W. Innys, 1730).
2. G. Gamow, "Zur Quantentheorie de Atomkernes," Z. Phys. **51**(3-4), 204–212 (1928).
3. B. R. Johnson, "Theory of Morphology-Dependent Resonances - Shape Resonances and Width Formulas," J. Opt. Soc. Am. A **10**(2), 343–352 (1993).
4. G. Binning, H. Rohrer, C. Gerber, and E. Weibel, "Surface Studies by Scanning Tunneling Microscopy," Phys. Rev. Lett. **49**(1), 57–61 (1982).
5. L. Esaki, "New Phenomenon in Narrow Germanium Para-Normal-Junctions," Phys. Rev. **109**(2), 603–604 (1958).
6. A. Lewis, M. Isaacson, A. Harootunian, and A. Muray, "Development of a 500-a Spatial-Resolution Light-Microscope. 1. Light Is Efficiently Transmitted through Gamma-16 Diameter Apertures," Ultramicroscopy **13**(3), 227–231 (1984).
7. D. W. Pohl, U. C. Fischer, and U. T. Durig, "Scanning near-Field Optical Microscopy (Snom)," J. Microscopy-Oxford **152**, 853–861 (1988).
8. W. M. Robertson, J. Ash, and J. M. McGaugh, "Breaking the sound barrier: Tunneling of acoustic waves through the forbidden transmission region of a one-dimensional acoustic band gap array," Am. J. Phys. **70**(7), 689–693 (2002).
9. C. Sias, A. Zenesini, H. Lignier, S. Wimberger, D. Ciampini, O. Morsch, and E. Arimondo, "Resonantly enhanced tunneling of Bose-Einstein condensates in periodic potentials," Phys. Rev. Lett. **98**(12), 120403 (2007).
10. E. A. Ash, and G. Nicholls, "Super-Resolution Aperture Scanning Microscope," Nature **237**, 510 (1972).
11. H. G. Winful, "Tunneling time, the Hartman effect, and superluminality: A proposed resolution of an old paradox," Phys. Rep.-Rev. Sec. Phys. Lett. **436**, 1–69 (2006).
12. L. A. Vainshtein, *Open resonators and open waveguides* (Golem Press, Boulder, Colo., 1969).
13. A. Kurs, A. Karalis, R. Moffatt, J. D. Joannopoulos, P. Fisher, and M. Soljacic, "Wireless power transfer via strongly coupled magnetic resonances," Science **317**(5834), 83–86 (2007).
14. G. Roll, T. Kaiser, S. Lange, and G. Schweiger, "Ray interpretation of multipole fields in spherical dielectric cavities," J. Opt. Soc. Am. A **15**(11), 2879–2891 (1998).
15. D. W. Vernooy, V. S. Ilchenko, H. Mabuchi, E. W. Streed, and H. J. Kimble, "High-Q measurements of fused-silica microspheres in the near infrared," Opt. Lett. **23**(4), 247–249 (1998).
16. D. K. Armani, T. J. Kippenberg, S. M. Spillane, and K. J. Vahala, "Ultra-high-Q toroid microcavity on a chip," Nature **421**(6926), 925–928 (2003).
17. R. K. Chang, and A. J. Campillo, eds., *Optical Processes in Microcavities* (World Scientific Publishing Co. Pte. Ltd., Singapore, 1996).
18. M. Oxborrow, "Traceable 2-D finite-element simulation of the whispering-gallery modes of axisymmetric electromagnetic resonators," IEEE Trans. Microw. Theory Tech. **55**(6), 1209–1218 (2007).
19. S. M. Spillane, T. J. Kippenberg, and K. J. Vahala, "Ultralow-threshold Raman laser using a spherical dielectric microcavity," Nature **415**(6872), 621–623 (2002).
20. L. Yang, T. Carmon, B. Min, S. M. Spillane, and K. J. Vahala, "Erbium-doped and Raman microlasers on a silicon chip fabricated by the sol-gel process," Appl.Phys. Lett. **86**, (2005).

#114612 - $15.00 USD Received 22 Jul 2009; revised 3 Sep 2009; accepted 10 Sep 2009; published 8 Oct 2009

21. T. Carmon, H. Rokhsari, L. Yang, T. J. Kippenberg, and K. J. Vahala, "Temporal behavior of radiation-pressure-induced vibrations of an optical microcavity phonon mode," Phys. Rev. Lett. **94**(22), 223902 (2005).
22. I. S. Grudinin, A. B. Matsko, and L. Maleki, "Brillouin Lasing with a CaF2 Whispering Gallery Mode Resonator," Phys. Rev. Lett. **102**, (2009).
23. M. Tomes, and T. Carmon, "Photonic Micro-Electromechanical Systems Vibrating at *X*-band (11-GHz) Rates," Phys. Rev. Lett. **102**(11), 4 (2009).
24. T. J. Kippenberg, S. M. Spillane, and K. J. Vahala, "Kerr-nonlinearity optical parametric oscillation in an ultrahigh-Q toroid microcavity," Phys. Rev. Lett. **93**, (2004).
25. T. Carmon, and K. J. Vahala, "Visible continuous emission from a silica microphotonic device by third harmonic generation," Nat. Phys. **3**(6), 470 (2007).
26. T. Carmon, H. G. L. Schwefel, L. Yang, M. Oxborrow, A. D. Stone, and K. J. Vahala, "Static envelope patterns in composite resonances generated by level crossing in optical toroidal microcavities," Phys. Rev. Lett. **100**, (2008).
27. A. A. Savchenkov, A. B. Matsko, V. S. Ilchenko, D. Strekalov, and L. Maleki, "Direct observation of stopped light in a whispering-gallery-mode microresonator," Phys. Rev. A **76**, (2007).
28. M. Cai, and K. Vahala, "Highly efficient hybrid fiber taper coupled microsphere laser," Opt. Lett. **26**(12), 884–886 (2001).
29. B. E. A. Saleh, and M. C. Teich, *Fundamentals of Photonics* (Wiley, 1991), pp. 135–143.
30. "A movie is presented in the file "tomes dynamics of the electric field in the tunneling region near a dielectric sphere.avi."
31. K. J. Vahala, "Optical microcavities," Nature **424**(6950), 839–846 (2003).

1. Introduction

Three centuries ago Newton reported on light transmission through a gap between prisms [1]: a phenomenon that, much later, could be placed in the more general context of particle tunneling. As first described by Gamow [2], an alpha particle that does not have sufficient energy to climb over the nuclear potential, can, nonetheless, appear on the other side of the barrier; thereby escaping the nucleus as if it were digging a tunnel. Like these nuclear potentials [2], spherical dielectrics have a similar three dimensional [3D] potential for trapping light [3]. Here, we directly image light propagating, without being seen, through the tunneling region of such an optical potential well. Images of the forbidden gap, as well as an interferogram showing wave-front spiraling, present a visual picture of the tunneling process.

Tunneling is universal to wave physics because it originates when an evanescent field transfers energy through a barrier to a region where a propagating wave is allowed. Tunneling has been reported for electrical currents [4, 5], light [6, 7], sound [8], Bose-Einstein condensate [9], radio frequencies [RF] [10], and countless other physical phenomena. Studies in the optical domain include the question of tunneling velocity and superluminality [11], as well as energy leakage [12] from resonators. In the RF regime, wireless transfer of energy was recently demonstrated [13], benefiting from the slow decay of the evanescent wave. When a wavefunction exits a potential by tunneling through the surrounding barrier (e.g. a spherical barrier), it is expected that the intensity will appear to emerge not from the device boundary, but instead from a region located at the other side of the potential barrier, which can be distant from the device physical boundary [3]. Further, when leaving the barrier, the phase front can spiral as it propagates [14]. Observations of these processes in real space are presented here.

#114612 - $15.00 USD Received 22 Jul 2009; revised 3 Sep 2009; accepted 10 Sep 2009; published 8 Oct 2009

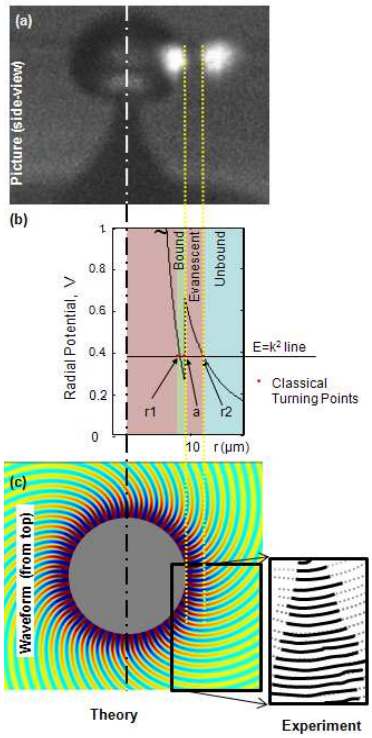

Fig. 1. (a) Picture of light escaping the cavity. Light on the left marks the bound circulating mode via forward scattering. Light on the right is the unbound radiation after passing through the evanescent region without being seen. There are no objects or surfaces at the place where light emerges on the right. (b) Graph of spherical-resonator potential vs. radius in the equatorial plane. Colors indicate whether the region is bound, unbound, or evanescent. The radius of the sphere is a. (c) Calculation of waveform outside of the cavity alongside experimental data. The dotted lines are a guide for the eye.

As a brief review of the theory, spherical dielectrics can trap light [15, 16] inside in a potential well (Fig. 1) near the surface. The energy can leave the well by tunneling through the centrifugal barrier that forms the outer wall of the potential well [3]. The electric field for the resonant mode in a spherical trap is shown in Fig. 2 and can be written in a spherical coordinate system as Eq. (1) [3, 17]:

$$\mathbf{E} \propto [\psi(kr)/kr][e^{i(m\phi-\omega t)}] \tag{1}$$

where the last term describes azimuthal propagation along the equator with m integer wavelengths resonating along the circumference at angular frequency ω. Here, k is the wavevector, r and ϕ are radial and azimuthal coordinates respectively. As derived in [15, 16], $\psi(kr)$ obeys the reduced radial Schrodinger equation (Eq. (2))

$$-\frac{d^2\psi(r)}{dr^2}+V(r)\psi(r)=E\psi(r), \tag{2}$$

where the energy $E=k^2$, and where, for a dielectric sphere in free space, the potential is $V(r)=k^2(1-n_{(r)}{}^2)+m(m+1)/r^2$ where $n_{(r)}$ is the refractive index (see Fig. 1(b) where the jump in radial potential at the dielectric-to-free-space interface is provided by the refractive index change from n to 1). Discussion of the similarities between the optical potential and the nuclear potential can be found in reference [3]. A calculation presented in Fig. 1(b) shows

#114612 - $15.00 USD Received 22 Jul 2009; revised 3 Sep 2009; accepted 10 Sep 2009; published 8 Oct 2009

how this potential implies an inner, classically-allowed well in the region r1<r<a (shown in green in Fig. 1(b) where the energy is larger than the potential and the optical wave is bound. This region is surrounded by classically-forbidden regions (E<V) in which the wave is evanescent in the radial direction. The outer-most region is another, classically-allowed region, in which the photons, upon tunneling, radiate away from the sphere. The points where E=V are called the classical turning points [3]. From experimental view, these turning points affect both phase and intensity. The phase is expected transition from having only azimuthal propagation (within the outer turning point) to having also a radial component, forming a spiral [14]. Measurable intensity is therefore expected to appear from a region after the most outer turning point leaving the tunneling region dark.

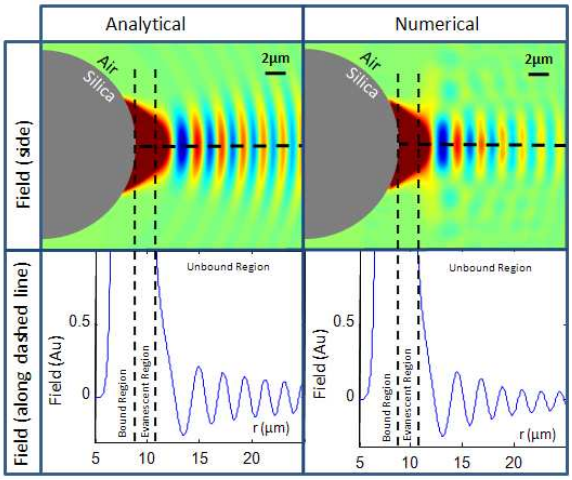

Fig. 2. Top: Analytical [3], and numerical solution to the field outside of the cavity in a transverse plane. Numerical solution calculated via finite element method as described in [18]. Bottom: The same field along the dashed line in the upper panels. A movie provided online shows that the field starts propagating radially only when crossing the outer turning point to the unbound region. (Media 1)

In the equivalent quantum-mechanical problem, a particle, such as the alpha particle, can spend time in the well and then tunnel through the classically forbidden region, a<r<r2 (shown in red in Fig. 1(b)), into the classically-allowed, free space (shown in blue in Fig. 1(b), far from the sphere. Similarly, light can spend some time in the dielectric potential before tunneling out. During this time, intensity in this inner classically allowed region is enhanced by multiple-recirculation and has been used in the past to allow low-threshold lasing [19, 20], vibration by centrifugal- [21] and compression-pressure of light [22, 23], parametric oscillation [24], third-harmonic generation [25], and modal studies [26, 27]. In such experiments, the tunneling rate is minimized by using relatively large dielectric diameters to support maximal recirculation and intensity enhancement.

2. Experiment

Our experiment (Fig. 1(a)) uses optical whispering galleries fabricated of silica-on-a-silicon-chip [16], and the optical wavelength is 1.5 μm. Light is evanescently coupled into the cavity via a tapered fiber with greater than 99% efficiency [28]. A side-view microscope with a 0.42 NA objective is used to image the emerging light as well as for mapping of the phase via interference with a plane-wave reference. The experiments were conducted with 1mW of input power. The cavity quality factors varied from 10^5 to 10^7 depending on cavity diameter. Typically, more than 95% of this power was coupled into the resonator as evident by less than

#114612 - $15.00 USD Received 22 Jul 2009; revised 3 Sep 2009; accepted 10 Sep 2009; published 8 Oct 2009

5% of the power transmitted via the output coupler. The tunneling was observed for all resonances.

2.1 Phasefronts

Calculations of the tunneling radiation [3], reveal that the phase fronts begin to spiral only after leaving the outer turning point (Fig. 1(c)) [14]. On the other hand, within that outer turning point, the phase fronts are flat planes passing through the origin of the dielectric. We measure this wavefront spiraling via interference with a reference plane wave. By moving a camera on a linear stage, we capture a series of images at different focal planes along the cavity side. In this manner an interferogram over a region outside of the external turning point is recorded and used to reconstruct the wavefront. Figure 1(c) shows the experimental results alongside the analytical solution.

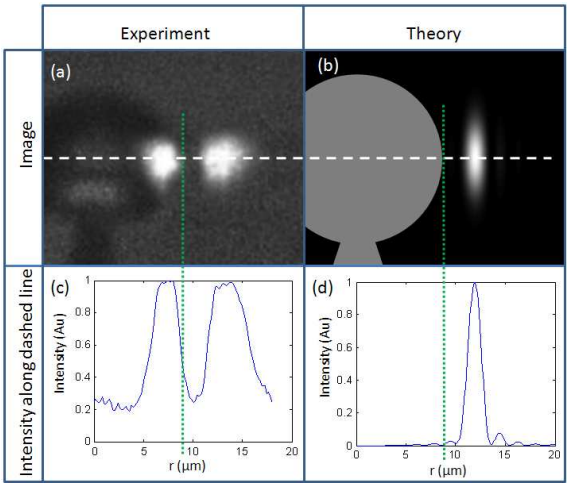

Fig. 3. (a) Side-view image of cavity showing the internal mode scattering at the dielectric boundary (left spot) and also emitting at the edge of the tunnel barrier (right spot). Light is coupled to the cavity via a tapered fiber at the far edge of the cavity, hidden by the resonator and out of focus due to distance. We verified that no light is scattered from the taper alone by careful examination without a nearby resonator. (b) Calculation of the expected intensity distribution as would be imaged by the microscope (no surface scattering is assumed) (c) Intensity along the line shown in (a). (d) Intensity along the line shown in (b).

2.2 Intensity

The expected field intensity is calculated (Fig. 2) and then an imaging integral [29] is performed in order to provide the image as seen by the camera (Fig. 3(b)). In more detail, the calculated cross sectional field [17, 18] is presented in Fig. 2. A movie presenting the dynamics of this electric field in time is provided [30]. The movie shows a side view of the resonator where color represents electric field. In both the bound and evanescent regions extending far from the resonator boundary (marked by a dotted line), the field has no radial motion. As the radially standing electric field inside oscillates between positive and negative, a node is born at the boundary between the unbound and evanescent zones and starts to propagate radially in the unbound zone. As seen in the movie, the peaks past this point move away from the resonator in the unbound region, instead of oscillating in place as the field in the evanescent region does.

A side view photomicrograph of the cavity is presented in Fig. 3(a). There are three important regions in the figure. Light circulating within the cavity is seen due to residual scattering at the dielectric interface. This scattering provides a convenient way to identify the physical boundary of the dielectric and therefore the inner, classical turning point. Light scattered from in the sphere is always present. Though some light is scattered in arbitrary

#114612 - $15.00 USD Received 22 Jul 2009; revised 3 Sep 2009; accepted 10 Sep 2009; published 8 Oct 2009

directions, most of the light is Rayleigh scattered in the forward direction. This results in clock-wise circulating modes appearing on our camera (Fig. 1(a)) to scatter light from their right-hand side while the light scattered from the left-hand side is propagating away from our microscope and is not reaching our camera; this is in agreement with previous experimental results [25]. As expected, changing the light to counter circulate caused the Rayleigh scattering (and the tunneling light) to switch to the other side in the image taken by the camera. While resonators containing fluorescent material emit light isotropically to produce an illuminated ring seen from all directions [20, 26, 27], our resonator is made of naked silica and produces mostly Rayleigh scattered light that can be viewed only from the forward side, (as in [25]). Beyond the cavity boundary in the micrograph, there is a dark region. This is the tunneling region. Finally, beyond the external classical turning point we see the emergence of light (out of "thin air" so to speak). As radiation from resonator is always propagating away from the resonator, it is not expected to be reflected from resonator. Reflection of the tunneled light and the Rayleigh scattered light were observed from the bottom silicon chip surface some 50 micron below and are out of the field of view in our images. The dark gap between the boundary of our device and the outer turning point is experimentally measured in Fig. 3(a) and calculated in Fig. 3(c) for comparison. Some deviation between the experimental and theoretical plots is believed to originate from the fact that the camera responsivity is not perfectly linear.

2.3 Tunneling distance

To further verify the tunneling process, the effect of microcavity diameter on the tunneling gap is measured and compared with theory. Figure 4 shows the data plotted alongside a theoretically calculated line. The data show a roughly linear increase in tunneling distance with respect to cavity diameter. The largest tunneling distance measured is 10 microns, which is observed for a cavity of 20 microns in radius.

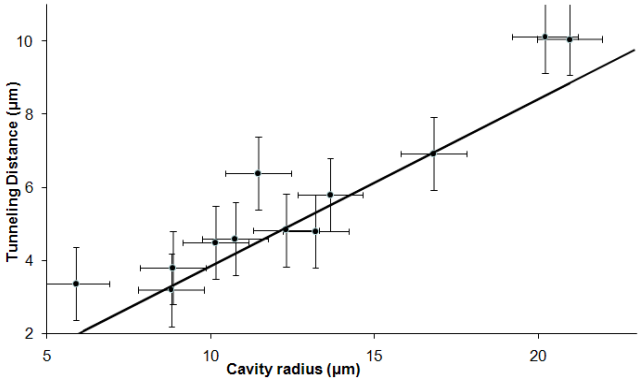

Fig. 4. Plot of tunneling distance vs. cavity radius with experimental results as points and calculation as a line.

3. Conclusion

Circular resonators that were previously used in various applications [17, 31] have allowed direct observation of the forbidden tunneling region as well as the measurement of phase fronts beyond the outer, classical turning point. The observations are striking as light escaping the radial dielectric potential appears to *emanate from nothing* in a region far beyond the physical boundaries of the device. Phasefront spiraling is recorded and resembles the spiraling of a water jet emerging from a sprinkler or spiraling galaxies in which an azimuthal component of velocity slows to conserve the angular momentum.

#114612 - $15.00 USD Received 22 Jul 2009; revised 3 Sep 2009; accepted 10 Sep 2009; published 8 Oct 2009